Synthesis of CdS quantum dots by the acidotolerant fungus *Trichoderma asperellum* and their potential in the flourescence detection of a leptospirosis-related oligomer

Kenworth Bryle P. Bal-iyang, Alexia Joanne F. Manuel, Don Joseph F. Rialubin, and Ronan Q. Baculi*

Department of Biology, College of Science, University of the Philippines Baguio City, Philippines

Quantum dots (QDs) are nanoparticles that exhibit the property of fluorescence. This unique optical property of QDs, coupled with their biocompatibility, has caused them to gain attention in biomedicine and be used in gene detection. In this study, cadmium sulfide (CdS) QDs were synthesized by the acidotolerant fungus *Trichoderma asperellum,* isolated from the main crater lake of Taal Volcano, Batangas, Philippines. UV-Vis and fluorescence spectrophotometry determined absorption maximum at 370 nm and emission maximum at 520 nm while size approximation determined a size of 2.52 nm. Zeta-potential analysis measured an average potential of -23.9 ± 3.39 mV. Optimization of reaction conditions revealed promotion of CdS QDs synthesis in the presence of phosphate at neutral conditions after 72 hours of incubation. Fluorescence detection assay conducted with a FAM-labeled leptospirosis-related oligomer demonstrated the occurrence of Forster Resonance Energy Transfer (FRET) when addition of CdS QDs resulted to fluorescence quenching. Fluorescence recovery after addition of the target oligomer, down to a concentration of 12 nM supports the use of CdS QDs for gene detection. However, further analysis showed that the detection was only able to differentiate the pyrimidine but not the purine single-base mismatched variant of the target oligomer. This study is the first report on *T. asperellum's* biosynthesis of CdS QDs.

*Corresponding author
Email Address: rqbaculi@up.edu.ph
Date received: January 31, 2020
Date revised: March 28, 2020
Date accepted: May 4, 2020

KEYWORDS

CdS Quantum Dots, fluorescence detection, leptospirosis, *Trichoderma asperellum*, mismatched variants

INTRODUCTION

Quantum dots (QDs) are an emerging class of nanoparticles, which exhibit the property of fluorescence as a result of quantum confinement effects. Coupled with their size in the nanoscale, this unique optical property of QDs has caused them to gain attention and be applied in various fields such as the industry, electronics, biomedicine, and pharmaceuticals (Lopez-Serrano et al. 2013; Jovin 2003).

Ranging from two to ten nanometers (nm) in diameter, QDs are composed of an innermost core, a middle layer shell, and an outermost cap (Medintz et al. 2005; Ghasemi et al. 2009). The semiconductor core is typically composed of cadmium sulfide (CdS), cadmium selenide (CdSe), or cadmium telluride (CdTe). This layer is responsible for majority of the QDs' properties, including their fluorescence. The shell, meanwhile, is often composed of zinc sulfide (ZnS) and is responsible for containing the toxicity and maximizing the optical properties of the core (Jamieson et al. 2007; Ghaderi 2012). Finally, the cap is a coating of polymeric units, which is used to modify the core's

solubility. This layer also facilitates conjugation processes that are conducted on the QDs (Kidane et al. 2009; Iga et al. 2007).

One of the most prominent types of QDs are the cadmium sulfide (CdS) QDs. CdS QDs exhibit maximum absorbance at wavelengths 450 to 650 nm and maximum fluorescence at wavelength 360 to 370 nm. Just like the other QDs, when they increase in diameter during their growth, their characteristic fluorescence color transitions towards the less energetic side of the visible spectrum (*i.e.* from blue to red) (Ulloa et al. 2016).

The physical and chemical syntheses of QDs require high thermodynamic, economic, and environmental costs. In addition, most QDs produced using these methods present low biocompatibility, low sensitivity to pH and ionic strength, and low stability at high osmolarity conditions, thus affecting their potential applications (Bruna et al. 2019). Given these constraints, there is a growing interest in the use of green and eco-friendly approaches for the production of QDs intended for various technological applications. These green and sustainable approaches solved the typical dilemma faced during QDs chemical synthesis and also impart the novel properties of biocompatibility and enhanced stability and solubility to the nanoparticles (Wang and Wang 2014; Ulloa et al. 2016; Gallardo et al. 2014 ; Monras et al. 2012).

Several microorganisms have been reported to biosynthesize cadmium- based QDs and most processes reported to date involve the use of cell extracts or living cells during the synthesis. Most of these microorganisms are non-extremophilic bacteria and fungi which include *Escherichia coli, Bacillus licheniformis, Saccharomyces cerevisiae, Schizosaccharomyces pombe, Fusarium oxysporum*, and *Pleurotus ostreatus* (Bao et al. 2010b; Ahmad et al. 2002; Monras et al. 2012; Tripathi et al. 2014; Borovaya et al. 2015). With the aim of producing QDs with improved properties, focus is now being directed towards the isolation of microorganisms from extreme environments. Considering their natural mechanisms of adaptation and novel metabolic pathways, extremophiles could potentially serve as sources of catalysts for QD synthesis. The low-temperature biosynthesis of fluorescent semiconductor CdS using psychrotolerant bacteria isolated from Antarctica has been documented (Gallardo et al. 2014; Plaza et al. 2016). Recently, Bruna et al. (2019) reported that the halophilic bacterial strains under *Halobacillus* sp. isolated from Atacama Desert, Uyuni Salt Flat, and Dead Sea can biosynthesize Cd-QDs under high osmolarity conditions.

Acidophilic and acidotolerant microorganisms can withstand and grow at environments with pH less than or equal to 4. In their evolutionary trajectory, they have developed unique adaptations such as powerful proton pumps, impermeable membranes, and acid stable enzymes to thrive in extreme conditions where excess of hydrogen ions, often coupled with excess of metal ions, exists (Johnson 2007; Golyshina and Timmis 2005). As a result of their peculiar physiology, acidophilic and acidotolerant microorganisms have found their applications in the fields of mining, food industry, pharmaceuticals, medicine, and nanotechnology. Ulloa et al. (2016) reported the use of acidophilic bacterial strains from the genus *Acidithiobacillus* for the production of fluorescent CdS QDs with high biocompatibility, stability, solubility, and the newly reported property of acid tolerance. Moreover, Ulloa et al. (2018) reported the enhanced synthesis of CdS QDs by the acidophilic bacteria *Acidithiobacillus thiooxidans* in the presence of phosphate. Although several bacterial strains from acidic environments with the ability to synthesize CdS QDs have been documented, the use of acidophilic and acidotolerant fungal species for this purpose is currently less explored.

Fluorescence assay through QDs provides not just a rapid and simple but also a sensitive and economical, way to detect the presence of nucleic acids that may be employed for disease detection and diagnostics through sensing of virulence or unique genes of pathogenic organisms (Lu et al. 2011). In the Philippines, leptospirosis detection can be used as a model for this application of QDs. In particular, fluorescence assay can be utilized to detect the gene LA0202 of *Leptospira interrogans*, a newly discovered protein coding region of the leptospire that codes for a hemolysin protein, a biomolecule demonstrated to be possibly involved in the virulence of the disease (Victoriano et al. 2009; Ren et al. 2003; Yang et al. 2009).

Fluorescence assay often operates through fluorescence quenching, which involves two compounds that interact through FRET to decrease the level of fluorescence of one of them (Valeur 2001). When FRET takes place under the condition of close proximity, an excited fluorescent donor, transfers some of its absorbed energy to an acceptor quencher compound. This generally leads to a decrease in fluorescence of the donor and possible increase in fluorescence of the quencher. To detect nucleic acids, DNAs or RNAs are often conjugated with dyes that interact with quenchers (Gadella 2009; Helms 2008; Chou and Dennis 2015). Among the particles that are used as quenchers, QDs have been one of the most recent to attract attention. During FRET events, QDs can act as an acceptor or a donor. Zhou et al. (2008) utilized QDs as FRET donors in the detection of DNA. Meanwhile, Lu et al. (2011) and Feng et al. (2017) utilized CdS QDs as FRET acceptors to detect an HIV-related oligonucleotide in concentration as low as 1nM.

This study aimed to synthesize CdS QDs using the acidotolerant fungus *T. asperellum* isolated from Taal Volcano, Philippines via cadmium, sulfide, and glutathione supplementation. It also aimed to determine the effects of pH, incubation period, phosphate, and citrate on the biosynthesis of CdS QDs. Furthermore, we applied the resultant nanoparticles in the fluorescence detection of *Leptospira interrogans'* LA0202 gene and its single-based mismatched variants.

MATERIALS AND METHODS

Sample collection and isolation of acidotolerant/acidophilic microbes

In sterile water bottles, surface water samples were collected from the main crater lake of Taal Volcano, Batangas, Philippines (14° 0′ 7″ N, 120° 59′ 34″ E). In the site, the temperature, and pH were recorded. Enrichment culture was prepared by adding 10 mL of water sample to 90 mL of liquid medium (pH 2.3) composed of 0.02 g yeast extract, 0.5 g $MgSO_4$, 0.15 g $(NH_4)_2S0_4$, 0.10 g KCl, 0.01 g $Ca(N0_3)_2$, and 0.5 mL 500mM $FeSO_4$ (Johnson, 1995). The enrichment culture was incubated at 30 °C for five days and then plated on solid medium (Gallardo et al. 2014). Morphologically distinct colonies were selected and then purified. Pure cultures were transferred on slants and were maintained in glycerol for further utilization.

Biosynthesis of Cds QDs

Biosynthesis of CdS QDs was conducted following the method described by Ulloa et al. (2016) with some modifications. Each oxidative stress-resistant isolate was grown for five days in its respective growth medium at pH 2.3. After which, the isolates were centrifuged and resuspended in phosphate buffers of pH 7.25 with 25 mM of cadmium sulfate ($CdSO_4$), 500 mM sodium sulfide (NaS), and 10 mM of glutathione. The samples were incubated for 72 hours and then centrifuged at 10000 rpm for 5 minutes. After centrifugation, the pellets were washed twice with phosphate buffer of pH 7.25. Fluorescence of the supernatant and pellets were evaluated through a UV-

transilluminator (302 nm) and a microplate reader (Fluorostar Omega) by excitation at 360 nm.

To test for the effect of reaction components such as sodium sulfide, cadmium sulfate, glutathione, and fungal cells on the synthesis of CdS QDs, five different treatments, each with a reagent removed from the reaction mixture, were utilized for the synthesis. To test for the effect of medium on the synthesis of CdS QDs, distilled water, growth medium, and sodium citrate buffer of pH 7.8 were utilized for the synthesis. To test for the effect of incubation period and pH, biosynthesis in phosphate buffers was conducted for various incubation periods (12, 24, 48, and 72 hours) and pH (4.55, 7.25, 7.85), respectively. Fluorescence of the samples was evaluated by the same set of procedures described above (Gallardo et al. 2014; Ulloa et al. 2016).

Extraction of extracellularly-produced CdS QDs
Fifty mL of the CdS QDs-producing isolate was centrifuged at 10000 rpm for 5 minutes. After centrifugation, the pellets were washed twice with phosphate buffer of pH 7.25 and stored for characterization. As for the supernatant, they were syringe filtered twice and were stored for characterization and the fluorescence detection assay.

Characterization of CdS QD-synthesizing isolate
The single isolate that was able to synthesize CdS QDs was preliminarily described based on its morphological and biochemical characteristics. For macroscopic characterization, the colony pigmentation, form, diameter, elevation, and margin were noted. For microscopic characterization, morphological characterization of cells was conducted under the microscope. For the biochemical characterization, the isolate was subjected to catalase test, amylase test, and protease test (Gallardo et al. 2014).

Characterization of the synthesized CdS QDs
The synthesized CdS QDs were subjected to various characterization techniques. Absorption spectrum from 200 nm to 700 nm and fluorescence spectrum at 360 nm excitation of the purified CdS QDs was determined through a microplate reader (FLUOstar Omega) (Monras et al. 2012; Ulloa et al. 2016).
To determine the particle size and concentration of the CdS QDs synthesized, sizing and approximation curves generated by Yu et al. (2003) were utilized. Meanwhile, analysis of Zeta potential was conducted under ¼ scale, 50 V voltage and 7417 µS/cm specific conductance.

Acid tolerance of CdS QDs
To test for the acid tolerance of the synthesized CdS QDs, 100 µL of 660 nM purified CdS QDs was exposed to phosphate buffer solutions of pH 1 to 7. In adjusting the pH, 6 M HCl was used. The samples were then incubated at 25°C for a period of 60 minutes. The fluorescence of each sample at 520 nm was determined using a microplate reader (FLUOstar Omega).

Molecular identification of CdS QD-synthesizing isolate
Pure culture of the biosynthesizing isolate was sent to Macrogen, South Korea for the amplification and sequencing of ITS1 and ITS4. Gene sequencing was performed using Big Dye Terminator v3.1 Cycle Sequencing Kit (Applied Biosystems, USA) and evaluation of the sequences and removal of low quality regions were done using ChromasPro software (http://www.technelysium.com). The DNA sequences were analyzed using NCBI BLAST (Basic Local Alignment Search Tool) software (http://blast.ncbi.nlm.nih.gov). Reference sequences from the GenBank database were used for multiple alignments using Muscle. Using the Tamura-Nei model of MEGA X, a phylogenetic tree was constructed by utilizing the Maximum Likelihood method (Tamura and Nei 1993) and Bootstrap analysis was used to evaluate the generated phylogenetic tree.

Synthesis of LA0202-related oligomer and its mismatched variants
The 200051st to the 200080th nucleotide bases of *Leptospira interrogans* serovar Lai str. 56601 (strain: 56601, serovar: Lai)'s chromosome one, which corresponds to the first 30 nucleotide bases of the LA0202 gene, was utilized in this study. Five single stranded oligonucleotides, shown below, were chemically synthesized by Macrogen, South Korea (https://dna.macrogen.com/kor/support/oligo/guide/price_info.jsp). The first oligomer (P), labelled with FAM dye, corresponds to the parent strand. The second oligomer (T0) is the complementary target to P. The third and fourth oligomer (T1A, T1C) served as the single base mismatched variants of the target oligomer.

P 5' – FAM – ATG ATT TCT TAC ATA TCT CAT CCA ATT GCT – 3'
T0 5' – AGC AAT TGG ATG AGA TAT GTA AGA AAT CAT – 3'
T1A 5' – AGC AAT TGG ATG AGA AAT GTA AGA AAT CAT – 3'
T1C 5' – AGC AAT TGG ATG AGA CAT GTA AGA AAT CAT – 3'

Fluorescence detection of LA0202-related oligomer and its mismatched variants
Prior to the detection, 200 nM of P, 200 nM of T0, T1A, T1B, and T1C, and 660 nM of CdS QDs were prepared in 20 mM Tris-HCl buffer of pH 7.4. Six samples were utilized, each containing 40 µL of 200 nM P. The first sample, without CdS QDs, served as the control. The remaining five samples were added with 40 µL of 660 nM of CdS QDs. The second sample was left as is and served as a basis for fluorescence quenching in the absence of the target oligomer. The third, fourth, fifth, and sixth samples were supplemented with 40 µL of 200 nM T0, T1A, T1B, and T1C, respectively. All samples were added with the prepared Tris-HCl buffer until a final volume of 330 µL is reached. To test for difference in level of fluorescence, each sample was excited at 485 nm and the fluorescence at 520 nm was determined. Fluorescence intensity at 520 nm was recorded and fluorescence intensity change (FIC) of the third to sixth samples were derived using the formula: $FIC = F_T/F_0 - 1$, where F_0 is the fluorescence intensity of the second sample and F_T is the fluorescence intensity of the third to sixth samples (Lu et al. 2011; Feng et al. 2017).

To determine the sensitivity of the target oligomer's detection, varying T0 concentrations were employed for the fluorescence detection assay. Final reaction concentrations of 3.03 nM, 6.06 nM, 12.12 nM, and 24.24 nM of the target oligomer were used to assess the sensitivity of detection at 485 nm excitation.

Statistical analysis
The fluorescence detection assay and the test for its sensitivity were conducted in six replicates and the data obtained were used to derive the mean values, which will be expressed along with their corresponding standard deviation (mean ± SD). To test for the presence of significant difference, one-way analysis of variance (ANOVA) at α=0.01 was carried out using IBM® SPSS® (Statistical Package for the Social Sciences) Statistics version 25.0.

RESULTS AND DISCUSSION

Isolation and identification of CdS QD-synthesizing microbe
Water samples were collected from the main crater lake of Taal Volcano, Batangas, Philippines. The measured pH of the surface water was 2.05 and the surface water temperature was about 30°C. Physico-chemical analyses conducted on the surface

water of the main crater lake by Delmelle et al. (1998) and Hernandez et al. (2017) revealed high concentrations of sulfate, chloride, sodium, potassium, calcium, and magnesium. Both studies also revealed low pH ranging from 2.4 to 2.9 as a result of underwater volcanic activity.

Using different enrichment media, twelve bacterial and fungal isolates were cultured on the basis of their ability to withstand acidic conditions and iron-induced oxidative stress. The selected isolates were able to grow at pH 2 in the presence of 2.5 mM of iron (Fe^{2+}). These isolates were further screened for the synthesis of CdS QDs by exposing them to the presence of cadmium, sulfide, and glutathione. Synthesis of CdS QDs was evaluated through UV transillumination and fluorescence spectrophotometry. Only isolate UPB 2A.1 showed the ability to synthesize CdS QDs as indicated by the observed fluorescence of both its supernatant and pellet after three days of incubation. Based on phenotypic characterization (Table 1), ITS sequencing, and phylogenetic analysis (Figure 1), the isolate is closely related to *T. asperellum*, a fungus of the family Hypocreaceae. Basic alignment search of ITS1 sequence revealed 100% similarity with *T. asperellum* isolate CTCCSJ-G-DK40568.

Table 1: Phenotypic characteristics of the CdS QD synthesizing isolate

Parameter	Characteristics
Mycelium color	white (surface), pale yellow (reverse)
Spore color and shape	green and subglobose
Conidia color and shape	green and ellipsoidal
Hyphae	septate and branched
Colony form	filamentous
Colony elevation	crateriform
Colony margin	filiform
Diameter	5 to 14 mm
Catalase production	positive
Amylase production	positive
Protease production	positive
pH change of medium after incubation	from 2.28 to 1.98

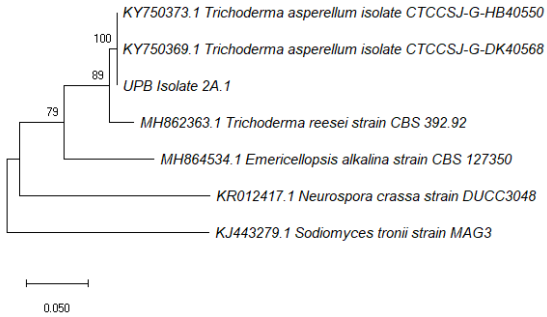

Figure 1: Phylogenetic tree based on ITS1 sequences, highlighting the phylogenetic position of the isolate relative to other *Trichoderma* isolates/species. *Emericellopsis alkalina*, *Neurospora crassa*, and *Sodiomyces tronii* were used as outgroups. The evolutionary history was inferred by using the Maximum Likelihood method based on the Tamura-Nei model. The tree is drawn to scale, with branch lengths measured in the number of substitutions per site. Evolutionary analyses were conducted in MEGA X.

The genus *Trichoderma*, predominantly found in soils, is present in a diverse array of habitats. Members of this phylogenetically diverse group are often utilized as biocontrol agents due to their mycoparasitic properties (Druzhinina et al. 2006). Numerous studies have already noted the acidotolerant and metal tolerant growth of *T. asperellum*. In a study conducted by Kawai et al. (2000), they were able to isolate and grow *T. asperellum* in media adjusted to pH levels ranging from 2.2 to 7.0 in the presence of a significant level of aluminum. *T. asperellum* was also isolated by Gillings et al. (2006) from an iron-containing groundwater source of pH 4.8 to 5.3. Finally, Singh et al. (2014) were able to culture *T. asperellum* under conditions of pH 4.0 to 8.0 in their study that determined the optimal growth condition of *Trichoderma* spp.

In this study, we observed a higher tolerance of *T. asperellum* to acidic conditions as manifested by its isolation in pH 2.05 and growth in medium of pH 1.98 to 2.28. The ability of *T. asperellum* to tolerate acid and/or metal-induced stress may be related to its broad tolerance to environmental extremes and its ability to produce resistant spores under stressful conditions.

The ability of *T. asperellum* to synthesize silver nanoparticles has been previously documented (Devi et al. 2013; Ahmed and Dutta 2019). Although several fungal species have demonstrated their ability to synthesize CdS QDs (Borovaya et al. 2015; Tripathi et al. 2014), no studies on *T. asperellum*'s ability to produce CdS QDs have been published yet. This is the first report on *T. asperellum*'s synthesis of CdS QDs through exposure to cadmium, sulfide, and glutathione at pH 7.25.

Optimization of conditions (reaction components, pH, incubation period and media) on the synthesis of CdS QDs

Extracellular and intracellular syntheses of CdS QDs were not attained in the absence of reaction components such as sodium sulfide, cadmium sulfate, or glutathione as indicated by the lack of visible fluorescence and the presence of a significant difference ($p<0.01$) with respect to the mixture with complete reaction components (Figure 2A and Figure 2B). While cadmium sulfate serves as a prerequisite source for the cadmium of the CdS QDs, the sulfide of the CdS QDs may not necessarily come from sodium sulfide. Sulfide may also be produced by the release of sulfate-reducing enzymes or by metabolism of glutathione (Gallardo et al. 2014). Monras et al. (2012) demonstrated that overexpression of *gshA* in *Escherichia coli*, the gene responsible for the synthesis of glutathione, facilitated CdTe QD synthesis. However, the lack of observed synthesis in the absence of sulfide indicates that the isolate cannot produce the required enzymes for sulfide generation; hence, the need for an external sulfide source. Aside from possibly providing a source of sulfide, glutathione allows the fungal cells to tolerate the presence of metals (Ulloa et al. 2016, Gallardo et al. 2014). Death of cells in its absence due to oxidative stress may account for the lack of synthesis. Finally, the lack of extracellular synthesis in the absence of fungal cells supports that synthesis of CdS QDs is facilitated by the isolate and not just a product of a non-biosynthetic chemical reaction.

By exposing *T. asperellum* at pH 4.55, 7.25, and 7.85, we observed that the extracellular and intracellular syntheses of CdS QDs occurred only in neutral pH 7.25 and 7.85 but not in the weakly acidic pH 4.55. Although both extracellular and intracellular syntheses occurred at pH 7.25, there was a reduced intracellular synthesis observed at pH 7.85 (Figure 3). The absence of synthesis in pH 4.55 may be attributed to the acidotolerant growth of the isolate with optimum growth at pH 6.5 (Singh et al. 2014). In addition, metals have increased solubility at lower pH, (Chuan et al. 1996) hindering the precipitation of cadmium to form CdS QDs. Ulloa et al. (2016) reported the synthesis of CdS QDs at pH 3.5-7 by the acidophilic bacteria of the genus *Acidithiobacillus* which grow optimally at the aforementioned pH condition. However, no synthesis occurred at pH 2 and 3 and this may be associated with the increased solubility of cadmium at these more acidic conditions.

The exact mechanism of QD biosynthesis is still unknown. Bao et al. (2010a) hypothesized that the initial phase of CdTe QD synthesis in fungal cells is extracellular in nature. As oxidative

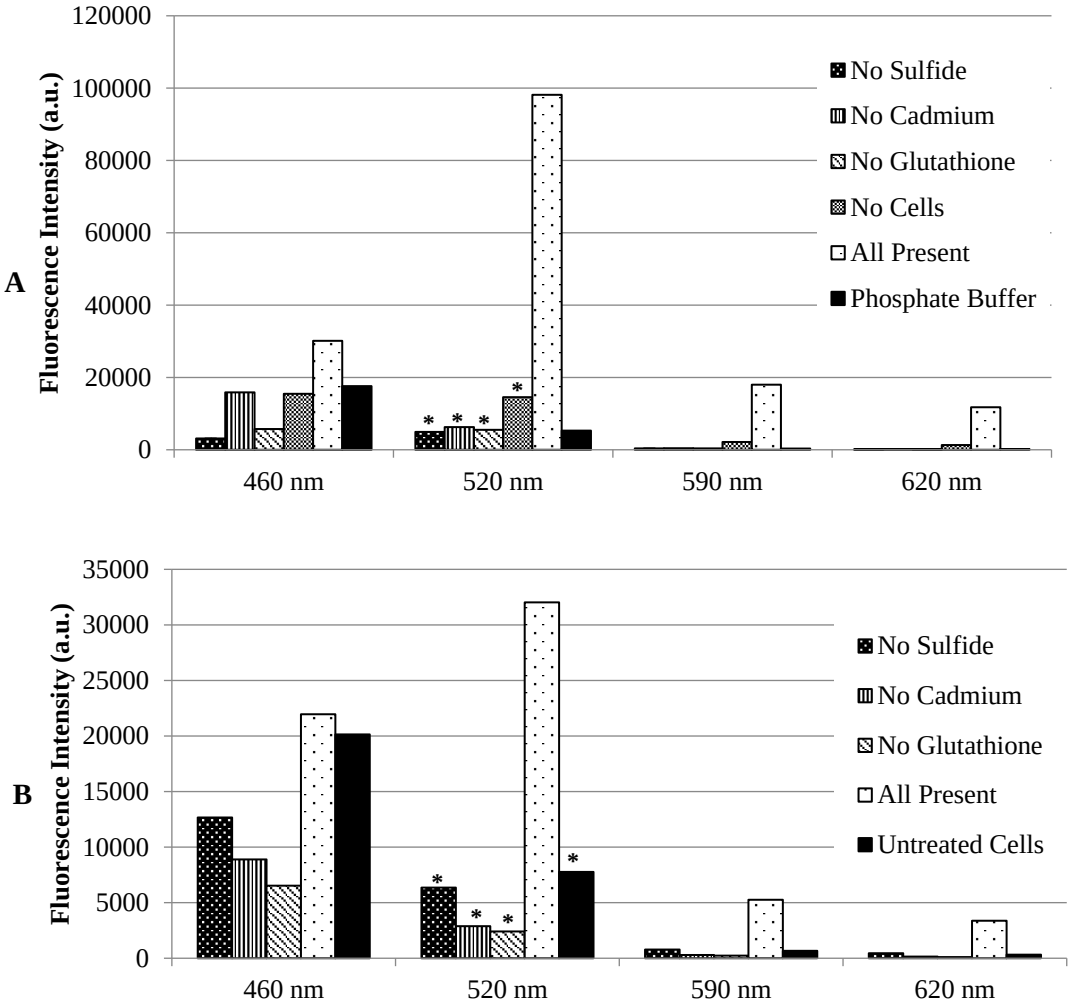

Figure 2: Effect of reaction components on the (A) extracellular and (B) intracellular synthesis of CdS QDs. Also presented is the fluorescence of cells that were not exposed to any of the reaction components.

* indicates presence of significant difference (P<0.01) at 520 nm emission with respect to the reaction mixture containing all the reagents being studied.

stress is imposed upon the cells by the cadmium ions, fungal cells release enzymes that coordinate the metal and the telluride to produce the CdTe QDs that are capped with biocompatible compounds. After extracellular synthesis, the CdTe QDs can then be taken in via endocytosis or other transport mechanisms and undergo intracellular growth via Ostwald ripening process. Meanwhile, Ahmad et al. (2002) proposed the possible use of sulfate-reducing enzymes by the filamentous fungus *Fusarium oxysporum* in the extracellular synthesis of CdS QDs. Reduction of intracellular synthesis in pH 7.85 may indicate the inability or difficulty of *T. asperellum* to endocytose at such condition.

Analysis done after exposing *T. asperellum* to the reaction conditions for 12, 24, 48, and 72 hours revealed an increase in fluorescence of supernatant and pellet with increasing length of incubation. Significant difference in both extracellular (Figure 4A) and intracellular (Figure 4B) with respect to the control was observed after 12, 24, 48, and 72 hours incubation. Maximum fluorescence of extracellularly and intracellularly produced CdS QDs was attained after 72 hours of incubation. The increase in fluorescence observed can be accounted for by the increased amount of time for *T. asperellum* to facilitate the synthesis of CdS QDs. However, we also observed that no significant change in the emission maximum was observed in the various lengths of time considered. This indicates that the CdS QDs produced by *T. asperellum* may not be size-tunable as they do not undergo growth with time to increase in size. This may be caused by the release of capping proteins that prevent Ostwald ripening from taking place (Sanklha et al. 2016). This report differs from that of several studies that showed ripening of biosynthesized CdS QDs from green to red (*i.e.* small to large QDs) (Gallardo et al. 2014; Ulloa et al. 2016; Mi et al. 2011; Monras et al. 2012).

Finally, the effect of media on the synthesis of CdS QDs was studied by exposing *T. asperellum* to different media, which include phosphate buffer, citrate buffer, the growth medium, and distilled water. CdS QD synthesis was only observed in phosphate buffer or citrate buffer as indicated by the presence of a significant difference with respect to the control (Figure 5). Phosphate and citrate ions increase the uptake of metals by facilitating the phosphate inorganic transport system and the metal/citrate-complex transport system, respectively. Ulloa et al. (2018) demonstrated that phosphate facilitates increased intracellular synthesis of CdS QDs in *Acidithiobacillus* by promoting cadmium uptake. They also determined that phosphate helps in alleviating cadmium-induced oxidative stress. Increased rate of CdS QD intracellular synthesis in the presence of phosphate indicates the possible involvement of proteins to support the phosphate inorganic transport system in the isolate (Van Veen et al. 1994). Citrate, on the other hand, supposedly increases intracellular CdS QD synthesis by forming tridentate complex with cadmium. The absence of significant difference on intracellular synthesis may indicate that the isolate possibly lacks the required transporter proteins for citrate-mediated

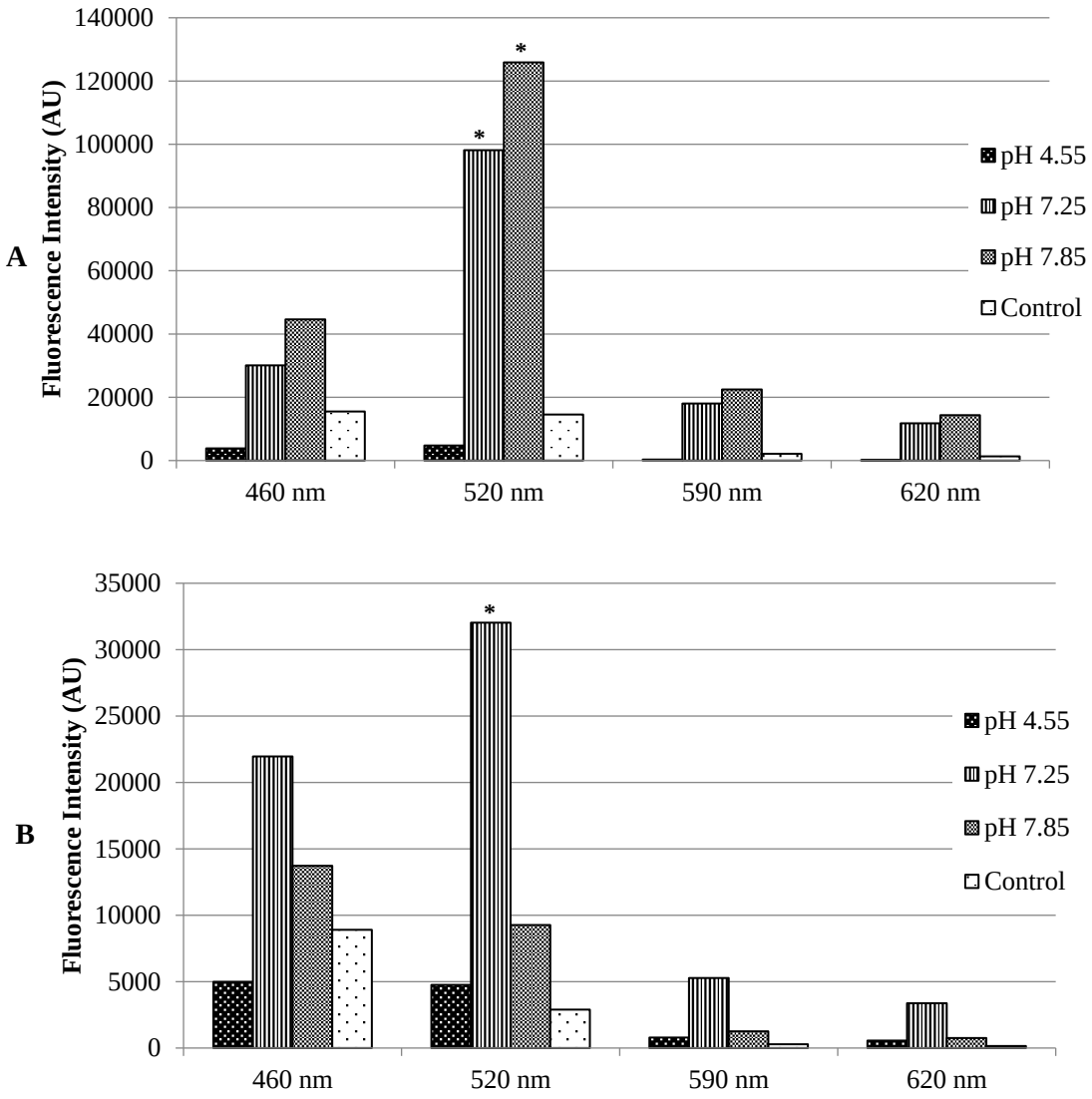

Figure 3: Effect of pH on the (A) extracellular and (B) intracellular synthesis of CdS QDs.
* indicates presence of significant difference (P<0.01) at 520 nm emission with respect to the control (at pH 7.25 in the absence of cadmium).

intracellular transport of cadmium (Krom et al. 2000; Gallardo et al. 2014). Absence of synthesis in the presence of the growth medium, with a measured pH of 1.98, can be accounted for by the aforementioned acidity-induced stress and increased solubility of cadmium at very low pH. This observation is not consistent with the results of Ulloa et al. (2016), where they recorded synthesis of CdS QDs by the acidophilic bacterium *Acidithiobacillus* in its growth medium.

Taking into consideration the effects of reaction components, pH, incubation period, and media, the optimal intracellular and extracellular syntheses of CdS QDs are attained by 72-hour exposure of *T. asperellum* to cadmium, sulfide, glutathione, and phosphate at pH 7.25.

Acid tolerance of CdS QDs

The pH tolerance of extracellularly-synthesized CdS QDs was determined by measuring the fluorescence spectra after exposure to various pH. The results showed that the fluorescence of the CdS QDs was significantly quenched at pH 1-2 and 4-5 but not at pH 3 and 6 with respect to the control at pH 7 (Figure 6).

Tolerance of the CdS QDs at pH 7 and 6 is a reflection of the optimum pH for growth of *T. asperellum* and the reaction condition. *T. asperellum* optimally grows at pH 6.5 (Singh et al. 2014) and the synthesis was undertaken at a pH of 7.25; hence, proteins released by the isolate to coordinate and cap the CdS QDs are anticipated to be optimal at neutral and weakly acidic conditions (Ahmad et al. 2002; Borovaya et al. 2015). Fluorescence degradation occurs when CdS QD is subjected to a pH level significantly lower than the pKa of the thiol group in its cap (Yang et al. 2016, Priyam et al. 2005); hence, pKa of the thiol groups that cap the CdS QDs may be higher than pH 6 and this may be responsible for the quenching at pH 1-2 and 4-5. The observed tolerance of the CdS QDs at pH 3 may be due to the release of another set of proteins with a very narrow tolerance to acidity. These proteins may be related to those utilized by the isolate to withstand its acidic growth medium. However, further studies are needed to verify the mechanism of this observed tolerance at pH 3.

Sankhla et al. (2016) showed that proteins play an important role in stabilizing CdS QDs. In the presence of proteins as capping agents, zeta potential of CdS QDs increases in magnitude, providing greater stability to avoid agglomeration and flocculation. In addition, proteins also help in restricting the size of CdS QDs by limiting Ostwald ripening. Acid tolerance of biosynthesized CdS QDs may be accounted for by the release of acid tolerant proteins that coordinate the synthesis and capping of CdS QDs (Ulloa et al. 2016). The biocompatibility and increased stability of acid tolerant CdS QDs produced by

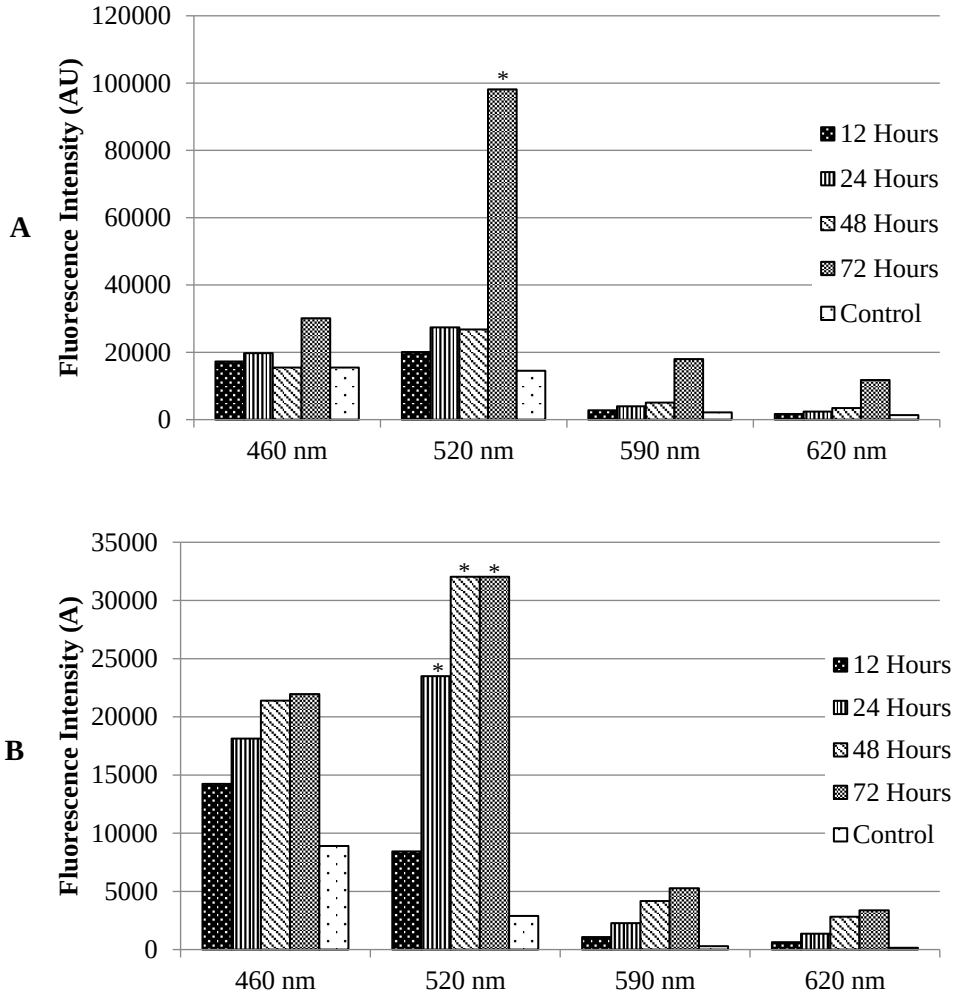

Figure 4: Effect of incubation period on the (A) extracellular and (B) intracellular synthesis of CdS QDs.
* indicates presence of significant difference (P<0.01) at 520 nm emission with respect to the control measured after 72 hours of incubation.

acidophilic and acidotolerant microorganisms permit their use in a wider array of applications in biomedicine.

Characterization of synthesized CdS QDs

UV-Vis analysis of the extracellularly-synthesized CdS QDs revealed maximum absorbance at the 280 to 400 nm and minimal absorbance at 400 to 700 nm. The first excitonic absorption peak of the CdS QDs was observed at about 370 nm (Figure 7). This peak arises from quantum confinement effects that result from the assembly of CdS QDs. The determined peak agrees with the established value on the typical absorption peak of CdS QDs at about 360 nm (Ulloa et al. 2016; Gallardo et al. 2014). When increase in size of CdS QDs take place, the first excitonic absorption peak nears the visible region, leading to a decrease in the effects of quantum confinement and band energy (Ulloa et al. 2016). Using the first excitonic absorption peak, an approximate of the particle size, extinction coefficient, and particle concentration can be derived from available sizing and approximation curves (Yu et al. 2003). Given a peak of 370 nm, an estimated CdS QD diameter of 2.52 nm was calculated. On the other hand, an estimated CdS QD concentration of 660 nM was computed with an extinction coefficient of 181089.51 L/mol•cm and optical density of 0.12. The size of the CdS QDs approximated fits within the lower limit of the range of CdS QD size from 2 to 10 nm (Li et al. 2007).

On the other hand, fluorescence spectrophotometry analysis over four filters (460, 520, 590, and 620 nm) revealed emission peak at 520 nm after excitation at 355 nm (Figure 8-9). This peak, which was observed in both intracellularly- and extracellularly-synthesized CdS QDs, is in agreement with the possible emission spectra of CdS QDs from 450 to 650 nm. It also matches with the emission of CdS QDs synthesized by the acidophilic bacterium *Acidithiobacillus thiooxidans* from 470 nm to 550 nm (Ulloa et al. 2016). An emission maximum at 520 nm corresponds to a green fluorescence. However, supernatant and pellets obtained when exposed to UV light revealed a yellow fluorescence. We suspect the presence of an emission peak in between 520 nm and 590 nm, which may account for the observed color of fluorescence.

Table 2: Average zeta potential measurement of CdS QDs

Average Zeta Potential	Standard Deviation	Voltage	Specific conductance
-23.9 mV	±3.39 mV	50 V	7417 µS/cm

Average zeta potential of the extracellularly synthesized CdS QDs in phosphate buffer (pH 7.25) was determined to be -23.9 ± 3.39 mV (Table 2). Zeta potential ranging from -27.29 to -20.51 mV reveals that the stability of the extracellularly synthesized CdS QDs is within the threshold of delicate dispersion, where the negatively charged surface of the CdS QDs facilitates near moderate stability to prevent agglomeration (Riddick 1968). However, although stable when constantly shaken, prolonged period of storage of the CdS QDs in the absence of agitation showed traces of agglomeration. Sankhla et al. (2016) showed that at pH 7.25, protein- capped CdS QDs and

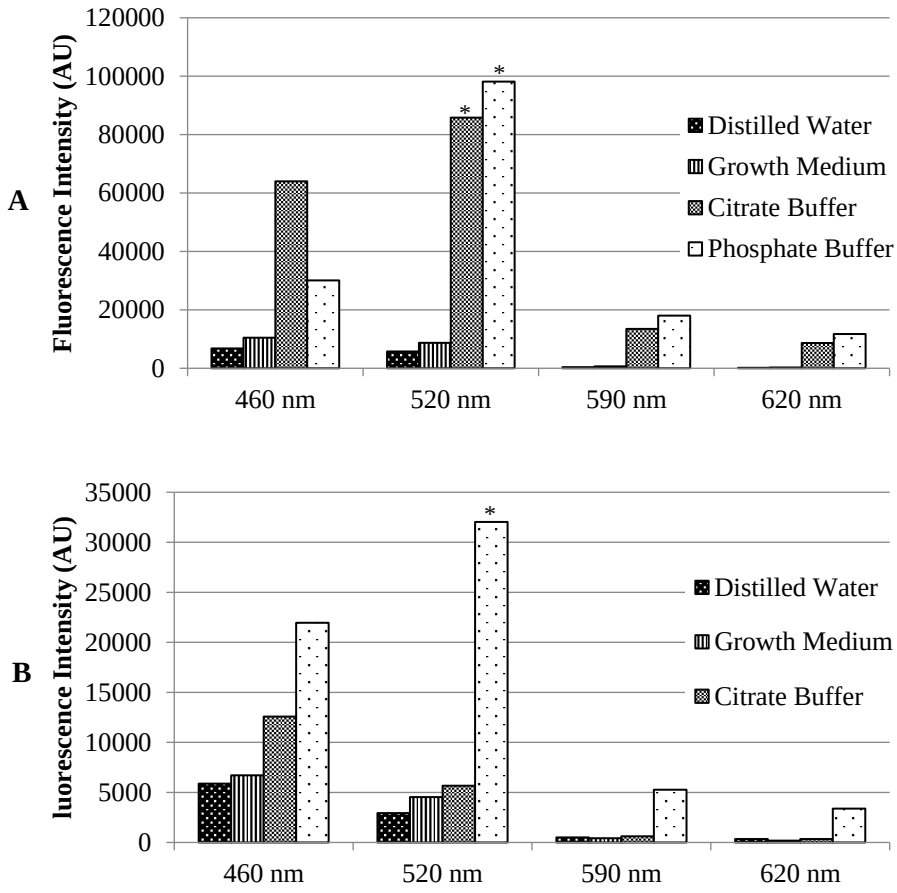

Figure 5: Effect of media on the (A) extracellular and (B) intracellular synthesis of CdS QDs.
* indicates presence of significant difference (P<0.01) at 520 nm emission with respect to the control (in phosphate buffer in the absence of cadmium).

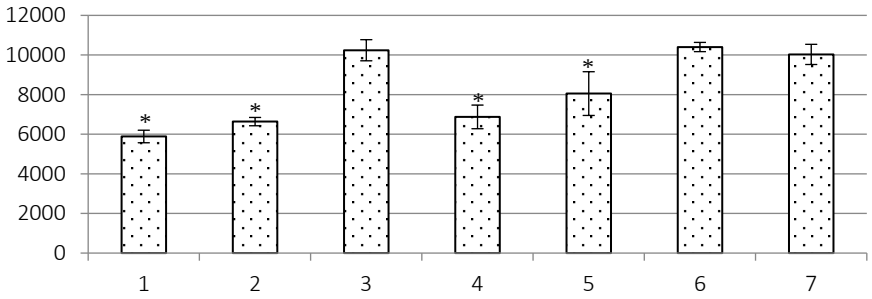

Figure 6: Effect of pH on the fluorescence of extracellularly synthesized CdS QDs. The assay was conducted in four replicates and repeated three times using 660 nM CdS QDs. Error bars represent the standard error while * denotes P-value (P<0.01) with respect to the control at pH 7.

uncapped CdS QDs have a zeta potential of -29 mV and -17.5 mV, respectively. The derived average zeta potential indicates that the CdS QDs are capped with biomolecules such proteins that allow their stabilization through electrostatic interaction. Presence of proteins as capping agents is supported by absorption maximum of the CdS QDs at 280 nm.

Fluorescence detection of a leptospirosis-related oligomer

The ability of CdS QDs to serve as donor and acceptor nanoparticles in FRET makes them suitable for FRET-based gene detection and disease diagnostic methods. In this study, extracellularly synthesized CdS QDs were employed in a fluorescence quenching and recovery assay to detect the presence of a Leptospirosis-related oligomer, a 20-mer portion of the hemolysin-coding gene LA0202, and its single-based mismatched variants. Different from the approach utilized by Lu et al. (2011) and Feng et al. (2017) that relied on CdS QDs as acceptor nanoparticles alone, this study utilized both the donor and acceptor properties of CdS QDs. CdS QDs and FAM-dye conjugated oligomer were excited at their maximum absorbance wavelength at 355 nm and 485 nm, respectively. After five minutes of incubation at 37°C, results of fluorescence quenching and recovery assay using CdS QDs as donor and acceptor nanoparticles, respectively, showed fluorescence quenching in the presence of the FAM-dye conjugated parent oligomer (P) and fluorescence recovery upon addition of the target oligomer (T0) (Figure 10).

FRET-based interaction of the CdS QDs and the FAM-dye-conjugated parent oligomer resulted in a significant fluorescence quenching with respect to the individual fluorescence of the parent oligomer and the CdS QDs alone. FRET occurs via non-radiative dipole-dipole coupling (Gadella 2009; Helms 2008; Chou and Dennis 2015), which is permitted by the adsorption of the parent oligomer on the CdS QDs. Although the CdS QDs have a negative zeta potential (23.9 ± 3.39 mV), coordination interaction of the nitrogenous backbone of the single-stranded

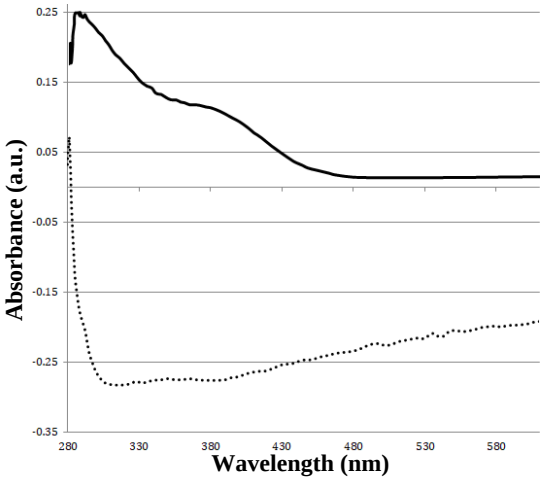

Figure 7: UV-Vis absorption spectrum of the extracellularly-synthesized CdS QDs (solid line) from 280 nm to 610 nm. The peak was observed at about 370 nm. Corresponding absorption spectrum of the control (dashed line) with no formed CdS QDs is also shown for comparison.

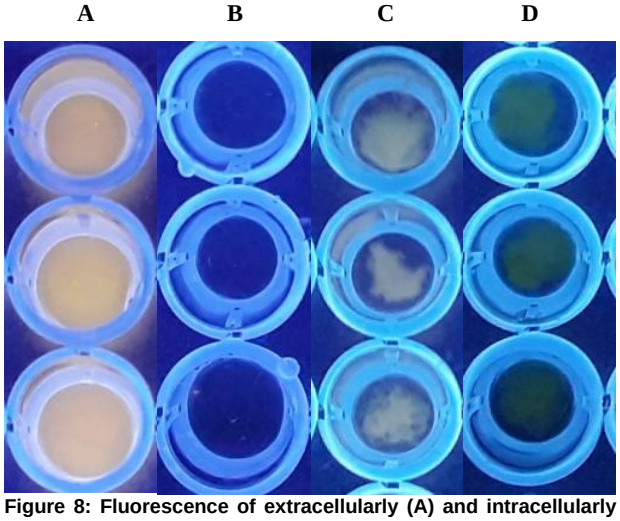

Figure 8: Fluorescence of extracellularly (A) and intracellularly (C) produced CdS QDs under UV transillumination. Corresponding controls without cadmium (B, and D) are also shown for comparison.

nucleic acid and the shell of the nanoparticle overcomes the repulsive forces to facilitate adsorption (Jian et al. 2010). In addition, FRET is permitted by an overlap and interaction of their respective absorption and emission spectra shown in Figure 11-12. CdS QDs serve as donor nanoparticles at 355 nm excitation and acceptor nanoparticles at 485 nm excitation. At 355 nm, CdS QDs are excited and are able to serve as donors of energy. On the other hand, at 485 nm, CdS QDs are at their ground state and are capable of accepting energy from donor molecules.

At 355 nm excitation, instead of fluorescing, the excited CdS QDs pass their absorbed energy to the FAM dye as they return to their ground state, causing about 50% reduction in the fluorescence of the nanoparticles. On the other hand, at 485 nm excitation, the excited FAM dyes pass their absorbed energy to the CdS QDs as they return to their ground state, leading to about 35% reduction in the fluorescence of the conjugated dye. These resulted to the significant fluorescence quenching observed in both 9A and 9B when the CdS QDs and the parent oligomer interacted with each other.

Addition of the target oligomer allowed base pairing with the single-stranded parent oligomer, which it perfectly complements with. This led to an increase in distance between the CdS QDs and the now-hybridized parent oligomer. As a result, significant recovery of fluorescence occurred as FRET can no longer be facilitated due to the absence of adsorption and coordination interaction between the CdS QDs and the parent oligomer. At 355 nm and 485 nm excitation, 57% and 91% of the quenched fluorescence was recovered, respectively (Figure 10).

In order to determine the selectivity of the fluorescence detection assay, we determined the degree of fluorescence recovery after addition of the target oligomer's single base-mismatched variants. Further analysis showed that the excitation at 355 nm and 485 nm were able to differentiate the pyrimidine (*i.e.* cytosine, TC) single-base mismatched variant due to the lack of significant fluorescence recovery. At 355 nm and 485 nm excitation, -5.4% and 45.2% of the quenched fluorescence was recovered, respectively. Interestingly, the assay revealed significant fluorescence recovery in the presence of the purine (*i.e.* adenine, TA) single-base mismatched variant. At 355 nm and 485 nm excitation, 54.6% and 95.5% of the quenched fluorescence was recovered, respectively. This agrees with the results of Lu et al. (2011), where their use of CdS QDs for detection of an HIV-related gene showed significant fluorescence recovery upon addition of the target oligomer, the purine (*i.e.* guanine) single-base mismatched variant, and the double-base mismatched variant. Only in the triple-base mismatched variant was significant fluorescence recovery not observed. The observed phenomenon furthers our recommendation on the use of highly specific and longer regions pertinent to the virulent gene for more accurate detection and diagnosis.

The sensitivity of the fluorescence detection assay was also evaluated at 485 nm excitation. Significant fluorescence recovery was attained in the presence of the target oligomer down to a final reaction concentration of 12.12 nM (Figure 13). At 24.24 nM and 12.12 nM, fluorescence recovery was 71.6% and 43.7%, respectively. On the other hand, at 6.06 nM and 3.03 nM, fluorescence recovery was 3.7% and -4.7%, respectively. 12.12 nM is much less than the 500 nM upper limit of detection determined by Feng et al.(2017) making the CdS QDs suitable for gene detection and disease diagnosis.

CONCLUSION

This study demonstrates the first report on *T. asperellum*'s synthesis of CdS QDs. Optimization of reaction conditions reveals that synthesis in the extracellular and intracellular level was enhanced at neutral conditions in the presence of cadmium, sulfide, glutathione, and phosphate after 72 hours of incubation. The synthesized CdS QDs displayed an absorption peak at 370 nm, emission peak at 520 nm, approximate size of 2.52 nm, and zeta potential of -23.9 ± 3.39 mV. Fluorescence detection assay conducted shows that the biosynthesized CdS QDs are able to serve as both acceptor and donor nanoparticles in FRET-based interactions to determine the presence of a leptospirosis-related target oligomer, down to a final reaction concentration of 12.12 nM, through significant recovery ($p<0.01$) of quenched fluorescence. Further studies should consider more intensive purification and characterization methods for both extracellularly- and intracellularly-synthesized Cds QDs and should focus on the optimization of the fluorescence detection assay. In addition, further investigation can be carried out on the differential selectivity of the assay towards purine and pyrimidine single-base mismatched variants of the target oligomer and its mechanism.

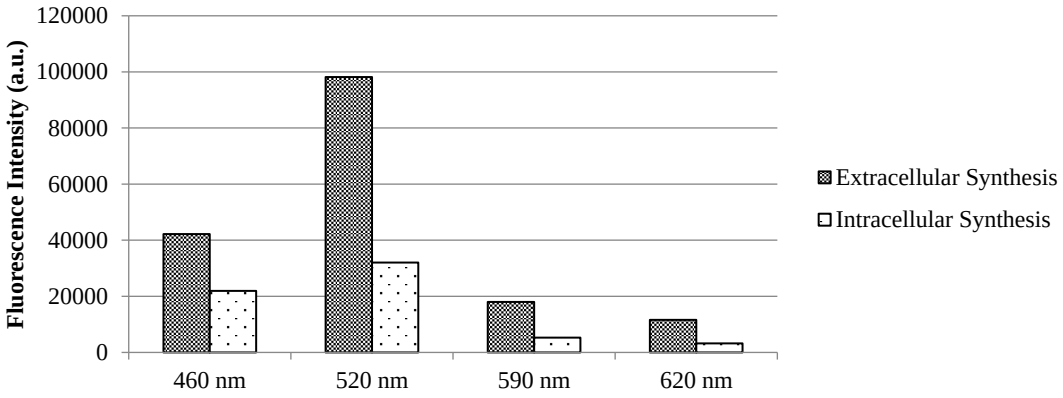

Figure 9: Fluorescence spectra of the extracellularly-synthesized and intracellularly-synthesized CdS QDs after excitation at 355 nm over four filters. The peak was observed at about 520 nm

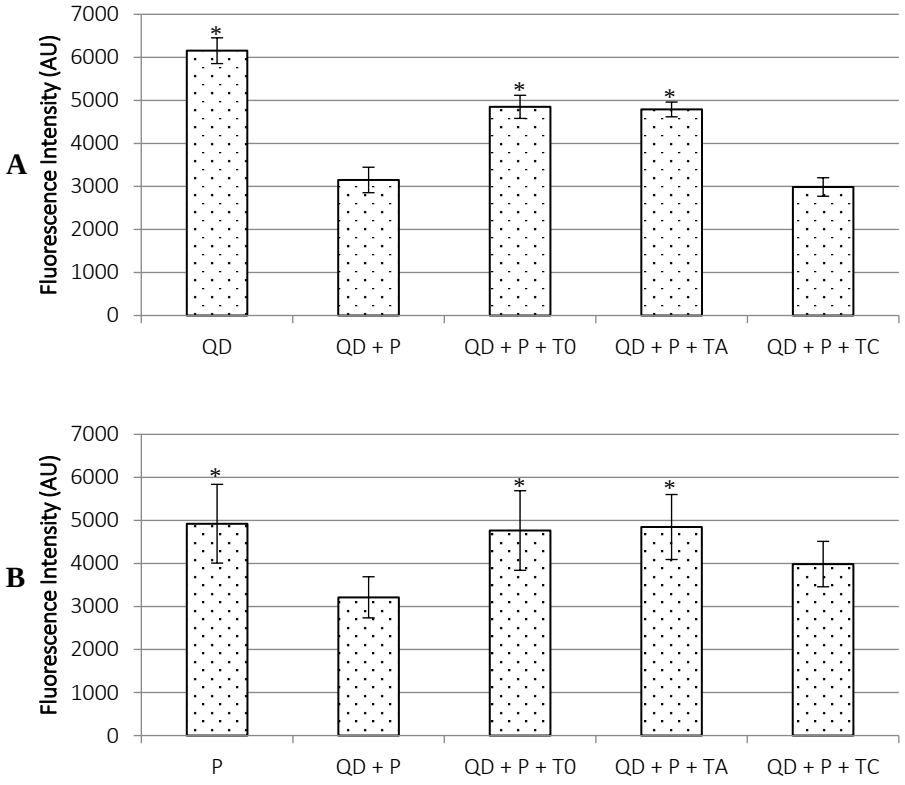

Figure 10: Fluorescence detection of a Leptospirosis-related oligomer (200 nM), the target oligomer, and its single-base mismatched variants (200 nM) using CdS QDs (660 nM) as (A) acceptor at 355 nm excitation and (B) donor nanoparticles at 485 nm excitation. The assay was conducted in six replicates and repeated three times. Error bars represent the standard error while * denotes P-value (P<0.01) with respect to the fluorescence of QD + P. P=Parent oligomer, T0=Target oligomer, TA=Adenine single-base mismatched variant, TC=Cytosine single-base mismatched variant.

CONFLICT OF INTEREST

The authors declare no potential conflicts of interests with respect to the research, authorship, and/or publication of this article.

REFERENCES

Ahmad A, Mukherjee P, Mandal D, Senapati S, Khan MI, Kumar R, Sastry M. Enzyme mediated extracellular synthesis of CdS Nanoparticles by the fungus, *Fusarium oxysporum*. J Am Chem Soc 2002; 124(41): 12108–12109.

Ahmed AA, Dutta, P. *Trichoderma asperellum* mediated synthesis of silver nanoparticles: characterization and its physiological effects on tea [*Camellia sinensis* (L.) Kuntze var. *assamica* (J. Masters) Kitam. Int J Curr Microbiol Appl Sci 2019; 8(4).

Bao H, Hao N, Yang Y, Zhao D. Biosynthesis of biocompatible cadmium telluride quantum dots using yeast cells. Nano Research 2010a; 3(7): 481–489.

Bao H, Lu Z, Cui X, Qiao Y, Guo J, Anderson JM, Li CM. Extracellular microbial synthesis of biocompatible CdTe quantum dots. Acta Biomater 2010b; 6(9): 3534–3541.

Borovaya M, Pirko Y, Krupodorova T, Naumenko A, Blume Y, Yemets A. Biosynthesis of cadmium sulphide quantum dots by using *Pleurotus ostreatus* (Jacq.) P. Kumm. Biotechnol Biotechnol Equip 2015; 29(6): 1156–1163.

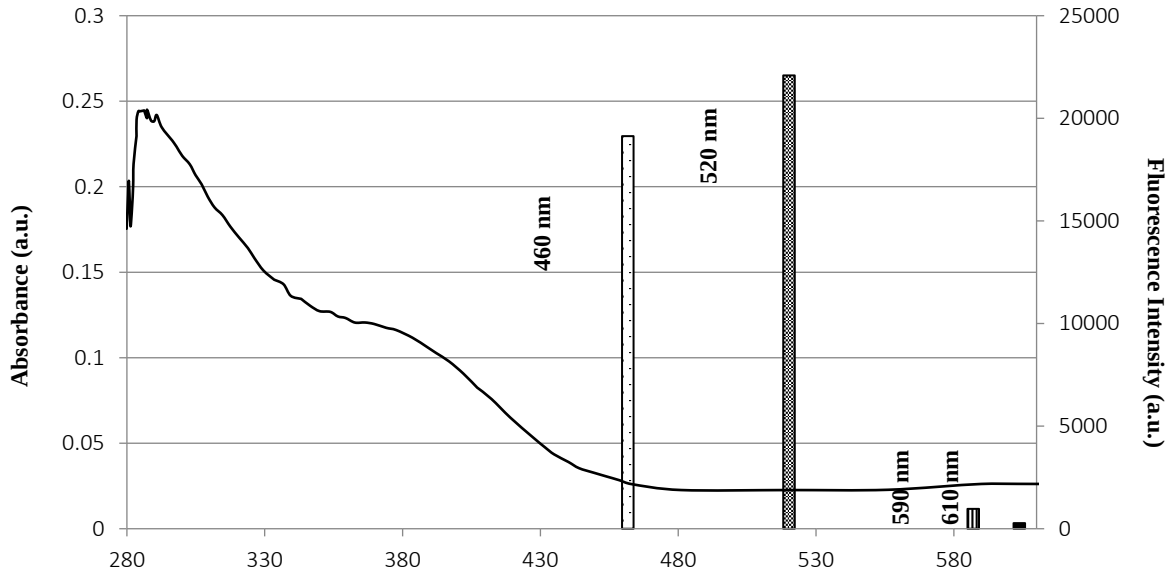

Figure 11: Relationship of the UV-Vis absorption spectrum of the extracellularly-synthesized CdS QDs and the fluorescence of FAM-dye-conjugated parent oligomer excited at 485 nm

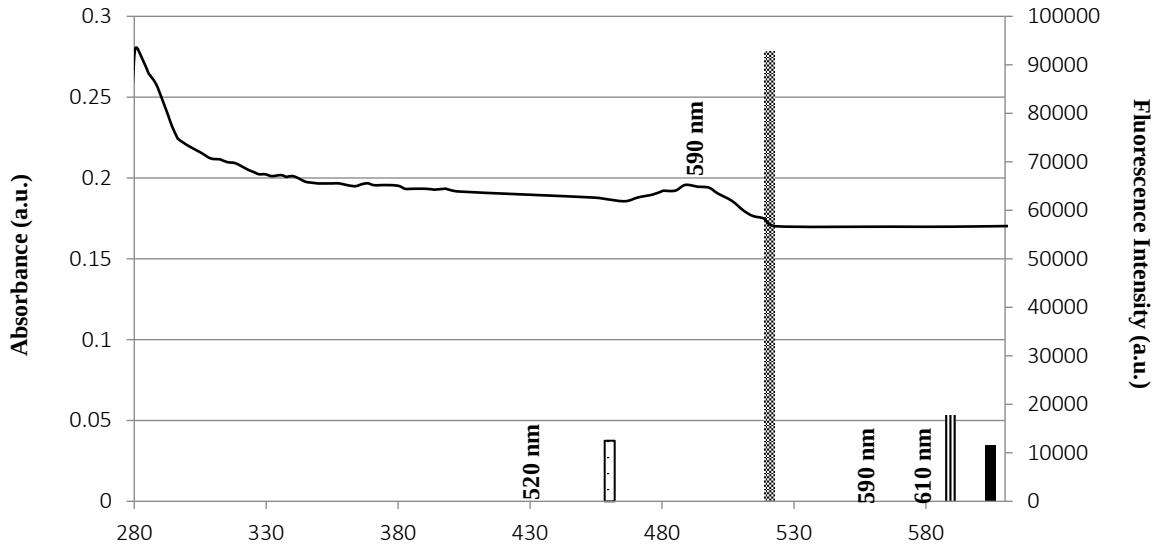

Figure 12: Relationship of the UV-Vis absorption spectrum of the FAM-dye-conjugated parent oligomer and the fluorescence of the CdS QDs excited at 355 nm

Bruna N, Collao B, Tello A. et al. Synthesis of salt-stable fluorescent nanoparticles (quantum dots) by polyextremophile halophilic bacteria. Sci Rep 2019; 9: 1953.

Chou K, Dennis A. Förster resonance energy transfer between quantum dot donors and quantum dot acceptors. Sensors 2015; 15(6): 13288–13325.

Chuan MC, Shu GY, Liu JC. Solubility of heavy metals in a contaminated soil: Effects of redox potential and pH. Water Air Soil Poll 1996; 90(3-4):543–556.

Delmelle P, Kusakabe M, Bernard A, Fischer T, de Brouwer S, del Mundo E. Geochemical and isotopic evidence for seawater contamination of the hydrothermal system of Taal Volcano, Luzon, the Philippines. Bull Volcanol 1998; 59 (8): 562–576.

Devi TP, Kulanthaivel S, Kamil D, Borah JL, Prabhakaran N, Srinivasa N. Biosynthesis of silver nanoparticles from *Trichoderma* species. Ind J Exp Biol 2013; 51.

Druzhinina IS, Kopchinskiy AG, Kubicek CP. The first 100 *Trichoderma* species characterized by molecular data. Mycoscience 2006; 47(2): 55–64.

Feng H, Liu S, Huang X, Ren R, Zhou Y, Song C, Qian D. Green biosynthesis of CdS nanoparticles using yeast cells for fluorescence detection of nucleic acids and electrochemical detection of hydrogen peroxide. Int J Electrochem Sci 2017; 12:618–628.

Gadella T. *FRET and FLIM techniques*. Amsterdam: Elsevier, 2009.

Gallardo C, Monrás JP, Plaza DO, Collao B, Saona LA, Durán–Toro V. Low-temperature biosynthesis of fluorescent semiconductor nanoparticles (CdS) by oxidative stress resistant Antarctic bacteria. J Biotechnol 2014; 187:108–115.

Ghaderi, S. Development of fluorescent nanoparticles 'quantum dots' for biomedical application (doctorate thesis). UCL Center for Nanotechnology and Regenerative Medicine

Division of Surgery and Interventional Sciences University College, London, 2012.

Ghasemi Y, Peymani P, Afifi S. Quantum dot: magic nanoparticle for imaging, detection and targeting. Acta Biomed 2009; 80(2):156–165.

Gillings MR, Holley MP, Selleck M. Molecular identification of species comprising an unusual biofilm from a groundwater treatment plant. Biofilms 2006; 3(01).

Golyshina OV, Timmis KN. Ferroplasma and relatives, recently discovered cell wall-lacking archaea making a living in extremely acid, heavy metal-rich environments. Environ Microbiol 2005; 7:1277–1288.

Helms V. Principles of computational biology: from protein complexes to cellular networks. Weinheim: Wiley-VCH Verlag GmbH & Co. KGaA, 2008.

Hernández PA, Melián GV, Somoza L, Arpa MC, Pérez NM, Bariso E, Solidum R. The acid crater lake of Taal Volcano, Philippines: hydrogeochemical and hydroacoustic data related to the 2010–11 volcanic unrest. Geol Soc 2017; 437 (1): 131–152.

Iga AM, Robertson JH, Winslet MC, Seifalian AM. Clinical potential of quantum dots. J Biomed Biotechnol 2007; (10): 76087.

Jamieson T, Bakhshi R, Petrova D, Pocock R, Imani M, Seifalian AM. Biological applications of quantum dots. Biomaterials 2007; 28(31): 4717–4732.

Jian J, Lin J, Xia C, Wen-Sheng Y, Tie-Jin L. Construction of CdS nanoparticle chain on DNA template. Chinese J Chemistry 2010; 21(2): 208–210.

Johnson DB. Physiology and ecology of acidophilic microorganisms. In C. Gerday and N. Glansdorff (eds.), Physiology and biochemistry of extremophiles.Washington, DC: ASM Press, 2007.

Johnson DB. Selective solid media for isolating and enumerating acidophilic bacteria. J Microbiol Met 1995; 23(2): 205–218.

Jovin TM. Quantum dots finally come of age. Nat Biotechn 2003; 21(1): 32–33.

Kawai F, Zhang D, Sugimoto M. Isolation and characterization of acid- and Al-tolerant microorganisms. FEMS Microbiol Lett 2000; 189(2): 143–147.

Kidane AG, Burriesci G, Edirisinghe M, Ghanbari H, Bonhoeffer P, Seifalian AM. A novel nanocomposite polymer for development of synthetic heart valve leaflets. Acta Biomater 2009, 5(7): 2409–17.

Kowshik M, Deshmukh N, Vogel W, Urban J, Kulkarni SK, Paknikar KM. Microbial synthesis of semiconductor CdS nanoparticles, their characterization, and their use in the fabrication of an ideal diode. Biotechnol Bioeng 2002; 78: 583–588.

Krom BP, Warner JB, Konings WN, Lolkema JS. Complementary metalion specificity of the metal-citrate transporters CitM and CitH of *Bacillus subtilis*. J Bacteriol 2000; 182 (22): 6374–6381.

Li H, Shih WY, Shih WH. Synthesis and characterization of aqueous carboxyl-capped CdS quantum dots for bioapplications. Ind Eng Chem Res 2007; 46(7): 2013–2019.

Lopez-Serrano A, Olivas RM, Landaluze JS, Camara C. Nanoparticles: A global vision. Characterization, separation, and quantification methods. Potential environmental and health impact. Royal Soc Chem 2013; 6(1): 38–56.

Lu W, Qin X, Luo Y, Chang G, Sun X. CdS quantum dots as a fluorescent sensing platform for nucleic acid detection. Microchimica Acta 2011; 175(3–4): 355–359.

Medintz IL, Uyeda HT, Goldman ER, Mattoussi H. Quantum dot bioconjugates for imaging, labelling and sensing. Nat Mater 2005; 4(6): 435–446.

Mi C, Wang Y, Zhang J, Huang H, Xu L, Wang S. Biosynthesis and characterization of CdS quantum dots in genetically engineered *Escherichia coli*. J Biotech 2011; 153 (3–4): 125–132.

Monras JP, Díaz V, Bravo D, Montes RA, Chasteen TG, Osorio-Román IO. Enhanced glutathione content allows the in vivo synthesis of fluorescent CdTe nanoparticles by *Escherichia coli*. PLoS ONE 2012; 7(11), e48657.

Plaza DO, Gallardo C, Straub YD, Bravo D, Pérez-Donoso JM. Biological synthesis of fluorescent nanoparticles by cadmium and tellurite resistant Antarctic bacteria: exploring novel natural nanofactories. *Microb Cell Fact* 2016; 15: 1.

Priyam, A, Chatterjee A, Das SK, Saha A. Synthesis and spectral studies of cysteine-capped CdS nanoparticles. Res Chem Interm 2005; 31(7-8): 691–702.

Ren SX, Fu G, Jiang XG, Zeng R, Miao YG, Xu H. Unique physiological and pathogenic features of *Leptospira interrogans* revealed by whole-genome sequencing. Nature 2003; 422(6934): 888–893.

Riddick T. Control of colloid stability through zeta potential: with a closing chapter on its relationship to cardiovascular disease. USA: Livingston Pub. Co, 1968.

Sankhla A, Sharma R, Yadav RS, Kashyap D, Kothari SL, Kachhwaha S. Biosynthesis and characterization of cadmium sulfide nanoparticles – An emphasis of zeta potential behavior due to capping. Mat Chem Phys 2016; 170: 44–51.

Singh A, Shahid M, Srivastava M, Pandey S, Sharma A, Kumar V. Optimal physical parameters for growth of *Trichoderma* species at varying pH, temperature and agitation. Virology and Mycology 2014; 3(1).

Tamura K, Nei M. Estimation of the number of nucleotide substitutions in the control region of mitochondrial DNA in humans and chimpanzees. Mol Biol Evol 1993;

Tripathi RM, Bhadwal AS, Singh P, Shrivastav A, Singh MP, Shrivastav BR. Mechanistic aspects of biogenic synthesis of CdS nanoparticles using *Bacillus licheniformis.* Adv Nat Sci: Nanosci Nanotech 2014; 5(2):025006.

Ulloa G, Collao B, Araneda M, Escobar B, Álvarez S, Bravo D, Pérez–Donoso JM. Use of acidophilic bacteria of the genus *Acidithiobacillus* to biosynthesize CdS fluorescent nanoparticles (quantum dots) with high tolerance to acidic pH. Enzyme MicrobTechnol 2016; 95: 217–224.

Ulloa G, Quezada CP, Araneda M, Escobar B, Fuentes E, Álvarez SA. Phosphate favors the biosynthesis of CdS quantum dots in *Acidithiobacillus thiooxidans* ATCC 19703 by improving metal uptake and tolerance. Front Microbiol 2018; 9.

Valeur B. Molecular fluorescence: principles and applications. Weinheim: Wiley-VCH, 2001.

Van Veen HW, Abee T, Kortstee GJ, Konings WN, Zehnder AJB. Translocation of Metal phosphate via the Phosphate Inorganic Transport System of Escherichia coli. Biochem 1994; 33(7): 1766–1770.

Victoriano AFB, Smythe LD, Gloriani-Barzaga N, Cavinta LL, Kasai T, Limpakarnjanarat K. Leptospirosis in the Asia Pacific region. BMC Infect Dis 2009; 9(1).

Wang EC, Wang AZ. Nanoparticles and their applications in cell and molecular biology. Integr Biol (Camb) 2014; 6(1):9–26.

Yang Y, He H, Zhong Y, Qin JH. The functional classification of a hemolysin protein LA0202 in *Leptospira interrogans* strain Lai. Fudan Univ J Med Sci 2009; 36 (5): 519-512.

Yang Z, Lu L, Kiely CJ, Berger BW, McIntosh S. Biomineralized CdS quantum dot nanocrystals: optimizing synthesis conditions and improving functional properties by surface modification. Ind Eng Chem Res 2016; 55(43): 11235–44.

Yu W, Qu L, Guo W, Peng X. Experimental Determination of the Extinction Coefficient of CdTe, CdSe, and CdS Nanocrystals. Chem Mats 2003, 15(14): 2854–2860.

Zhou D, Ying L, Hong X, Hall EA, Abell C, Klenerman D. A compact functional quantum dot−DNA conjugate: preparation, hybridization, and specific label-free DNA detection. Langmuir 2008, 24(5): 1659–1664.